

Tests of models for saccade–vergence interaction using novel stimulus conditions

Arun N. Kumar · Yanning H. Han ·
Robert F. Kirsch · Louis F. Dell’Osso ·
W. Michael King · R. John Leigh

Received: 29 September 2005 / Accepted: 27 March 2006
© Springer-Verlag 2006

Abstract During natural activities, two types of eye movements – saccades and vergence – are used in concert to point the fovea of each eye at features of interest. Some electrophysiological studies support the concept of independent neurobiological substrates for saccades and vergence, namely saccadic and vergence burst neurons. Discerning the interaction of these two components is complicated by the near-synchronous occurrence of saccadic and vergence components. However, by positioning the far target below the near target, it is possible to induce responses in which the peak velocity of the vertical saccadic component precedes the peak velocity of the horizontal vergence component by ~ 75 ms. When saccade–vergence responses are temporally dissociated in this way, the vergence velocity waveform changes, becoming less skewed. We excluded the possibility that such change in skewing was due to

visual feedback by showing that similar behavior occurred in darkness. We then tested a saccade-related vergence burst neuron (SVBN) model proposed by Zee et al. in *J Neurophysiol* 68:1624–1641 (1992), in which omnipause neurons remove inhibition from both saccadic and vergence burst neurons. The technique of parameter estimation was used to calculate optimal values for responses from human subjects in which saccadic and convergence components of response were either nearly synchronized or temporally dissociated. Although the SVBN model could account for convergence waveforms when saccadic and vergence components were nearly synchronized, it could not when the components were temporally dissociated. We modified the model so that the saccadic pulse changed the parameter values of the convergence burst units if both components were synchronized. The modified model accounted for velocity waveforms of both synchronous and dissociated convergence movements. We conclude that both the saccadic pulse and omnipause neuron inhibition influence the generation of vergence movements when they are made synchronously with saccades.

Keywords Parameter estimation · Saccades · Vergence

A. N. Kumar · Y. H. Han · R. F. Kirsch · L. F. Dell’Osso ·
R. J. Leigh (✉)
Department of Biomedical Engineering,
Department of Veterans Affairs Medical Center and
University Hospitals, Case Western Reserve University,
11100 Euclid Avenue, Cleveland,
OH 44106-5040, USA
e-mail: rjl4@case.edu

L. F. Dell’Osso · R. J. Leigh
Department of Neurology,
Department of Veterans Affairs Medical Center and
University Hospitals,
Case Western Reserve University,
Cleveland, OH, USA

W. M. King
Department of Otolaryngology,
University of Michigan,
Ann Arbor, MI, USA

1 Introduction

In the visual environment, features of interest lie in different directions and at different distances. In order to achieve optimal, binocular vision, the fovea of each eye (corresponding to highest visual acuity) must be pointed at the feature of interest (Carpenter 1991). During visual search, two distinct types of eye movements move

the point of fixation of each eye from one feature to the next (Carpenter 1988; Leigh and Zee 2006; Mays 2003).

Saccades are rapid movements that rotate the eyes through similar angles and in the same direction (conjugate or versional movements). Premotor signals for saccades are generated by medium-lead burst neurons located in the brainstem reticular formation (van Gisbergen et al. 1981; Sparks 2002), which project monosynaptically to ocular motoneurons. Premotor burst neurons for horizontal saccades lie in the paramedian pontine reticular formation (PPRF) (Horn et al. 1997), whereas those for vertical saccades lie in the rostral interstitial nucleus of the medial longitudinal fasciculus (riMLF) in the midbrain (Horn and Büttner-Ennever 1998). The activity of both sets of premotor, saccadic burst neurons is controlled by omnipause neurons, which lie in the pontine nucleus raphe interpositus (Horn et al. 1994), and are tonically active except during saccades (Yoshida et al. 1999; Busetini and Mays 2003; Mays 2003).

Voluntary shifts of the line of sight between objects lying at different depths in the environment require vergence movements that rotate the eyes in opposite directions (disjunctive rotations). Although it is possible to make pure vergence movements, during natural behavior, vergence is usually accompanied by one or more saccades. Electrophysiological evidence indicates that the premotor signals for vergence shifts between two targets lying at different depths may be generated by midbrain “vergence burst neurons;” these cells receive weak inhibition from the omnipause neurons during the movement (Mays 1984; Mays et al. 1986; Mays and Gamlin 1995). Alternatively, at least a portion of the vergence may be produced by disjunctive saccades generated by different discharge of medium lead burst neurons that encode left or right eye movements (Zhou and King 1998; Sylvestre and Cullen 2003).

When human subjects make most combined saccade–vergence movements, the peak velocities of saccadic and vergence components occur at almost the same time (Zee et al. 1992). Furthermore, saccades and vergence movements made in combination alter each other’s properties. Thus, saccades made in combination with vergence are slowed down (compared with conjugate movements), whereas vergence movements are speeded up if they are made with a saccade (Collewyn et al. 1995; Zee et al. 1992). This co-dependence of the dynamic properties of saccades and vergence occurs even if vertical saccades are combined with horizontal vergence (Enright 1984). In this case, since vergence movements are horizontal but the saccades are vertical, it seems improbable that an interaction of vergence and saccadic commands in the ocular motor plant could account for

the speeding up of vergence. More likely, a central interaction between saccadic and vergence systems occurs.

We recently reported an experimental paradigm in which it was possible to temporally dissociate saccadic and vergence components (Kumar et al. 2005). Specifically, when subjects shifted fixation from a far target to a near target that was located higher, the peak velocity of the horizontal convergence component followed the peak velocity of the vertical saccadic by ~ 75 ms (“dissociated responses”). When subjects shifted fixation between a near target that was located lower than a far target (the more natural situation), the peak velocity of the horizontal convergence component followed the peak velocity of the vertical saccadic by ~ 12 ms (“near-synchronized responses”). Similar, but less marked, differences were found for divergence–saccade responses. One substantial difference between the two types of responses, apparent in every subject, was that the vergence component was less skewed during dissociated responses. The time taken for saccades to reach peak velocity did not show consistent changes under the two stimulus conditions, which would imply a specific change in the vergence dynamics. Thus, the median skewing ratio (time from onset to peak velocity/total duration) of vergence components was 0.27 for movements that were near-synchronized but 0.38 for responses that were dissociated (difference significant, $P < 0.001$). Representative responses are shown in Fig. 1.

These data provided us with an opportunity to test a current model for saccade–vergence interactions. In the “saccade-related vergence burst neuron” (SVBN) model described by Zee et al. (1992) (Fig. 2), vergence movements are speeded up when combined with a saccade because the discharge of the omnipause neurons is silenced, removing inhibition from both vergence and saccadic burst neurons. Note that, in the model, the only interaction between saccadic and vergence burst neurons is via the omnipause neurons. In humans, small ($\sim 0.2^\circ$), high-frequency (10–35 Hz) conjugate oscillations occur during saccade–vergence movements, and it has been proposed that they could be used as behavioral evidence that the omnipause neurons are inhibited (Ramat et al. 2005). In our prior study, we established that such oscillations occurred during both nearly synchronous and temporally dissociated saccade–vergence responses, suggesting that omnipause neurons were inhibited irrespective of the stimulus paradigm.

To test the SVBN model, we applied the techniques of parameter estimation to calculate optimal values of the model’s parameters for averaged responses from normal subjects as they made either near-synchronous or temporally dissociated saccade–vergence responses. We then used skewing of the convergence velocity profile

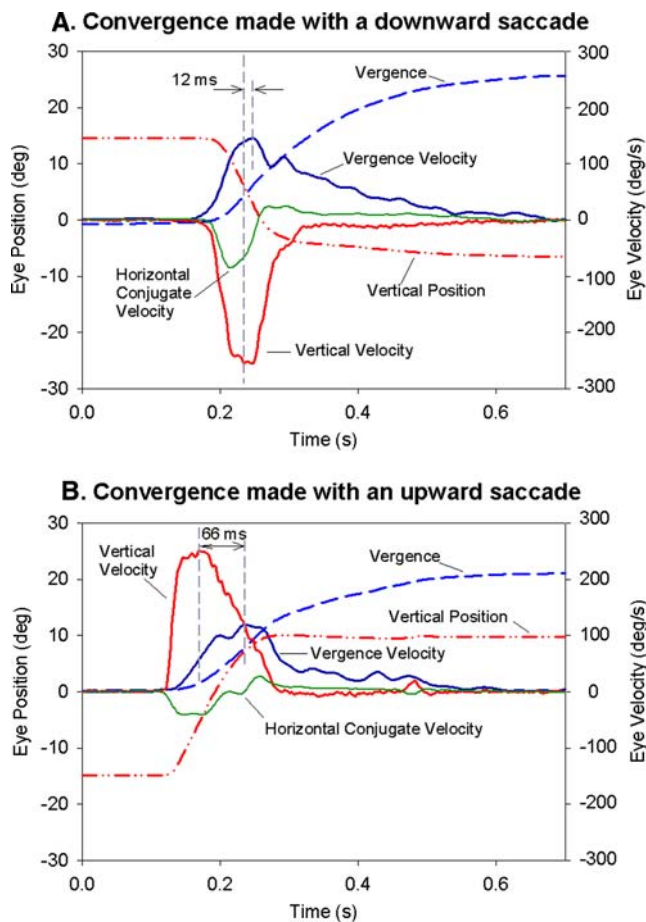


Fig. 1 Representative records from one subject comparing convergence movements made in association with either a downward saccade **a** or an upward saccade **b**. *Dashed gray vertical lines* indicate timing of peak vertical eye velocity and peak vergence velocity; dissociation periods are specified, being much greater for convergence made with an upward saccade. Note also the presence of high-frequency conjugate horizontal oscillations during these convergence–saccade responses

as the fiduciary, since this feature showed a robust difference for the two types of response (Kumar et al. 2005). We found that the SVBN model could not account for temporally dissociated responses, which led us to develop a new model, in which the parameters governing generation of the vergence component changed if it was nearly synchronized with a saccade. This revised model was able to simulate the velocity waveform of both types of convergence response.

2 Subjects and methods

We studied five healthy human subjects (four males, one female) whose ages ranged from 25–57 years, and whose responses were representative of ten subjects we have

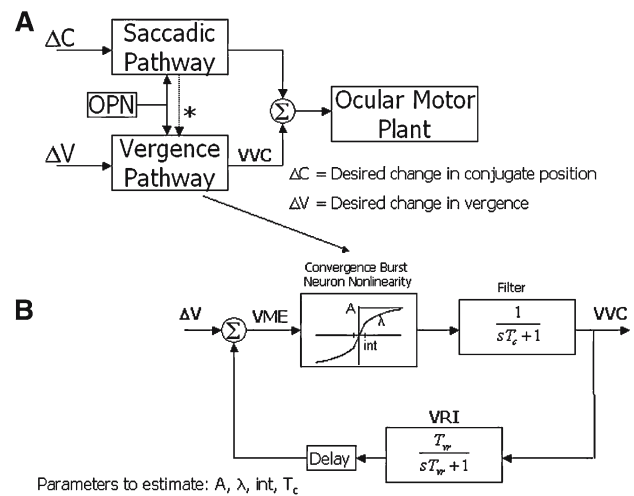


Fig. 2 **a** Simple schematic of saccade–vergence interaction, summarizing a fundamental concept of the saccade-related vergence burst neuron (SVBN) model by Zee et al. (1992). The interaction between saccadic and vergence pathways depends solely on the activity of omnipause neurons (OPN), which regulate neuron discharge in both component pathways (see text). The vergence velocity command (VVC) is generated by a pure vergence pathway summing with the SVBN pathway (activated by the omnipause neurons during combined saccade–vergence movements). The *dashed line by the asterisk* indicates the proposed modification to the SVBN model prompted by the results of the present study, whereby the saccadic system influences the parameters of the convergence system. **b** A more detailed view of the convergence subsystem and the parameters selected for estimation. In this modified SVBN model, a single pathway representing the convergence velocity neurons generates the VVC. The shape of the convergence nonlinearity is qualitatively similar to that of the saccadic system. The parameter values change if a saccade occurs synchronous with a convergence movement. *VME* vergence motor error, *VVC* vergence velocity command, *VRI* vergence resettable integrator, T_{vr} time constant of VRI, Delay vergence local feedback delay. See text for details

reported previously (Kumar et al. 2005). The study was conducted in accordance with the tenets of the Declaration of Helsinki and was approved by the Institutional Review Board of the Louis Stokes Cleveland Department of Veterans Affairs Medical Center. Eye movements were measured using the magnetic search coil technique. Visual targets consisted of a red laser spot projected onto a tangent screen at a viewing distance of 1.2 m (the “far target”) and a green light-emitting diode (LED) positioned at a distance of either 10 or 20 cm (the “near target”). Both near and far targets were positioned on the mid-sagittal axes of subjects’ heads, unless specified otherwise. Experimental paradigms were of two main types: (1) With the far target located lower than the near target – far–down near–up (FDNU), and (2) with the far target located higher than the near target – far–up near–down (FUND). Subjects made self-

paced shifts of the point of fixation between near and far targets for each of these two paradigms, under a variety of experimental conditions that are described in our prior paper (Kumar et al. 2005). For the present study, the arrangement of targets was as follows:

- (a) Far-down near-up (FDNU): Subjects were asked to make self-paced shifts between the far and near targets, which were both continuously illuminated. The direction of the near target was at up 10° and the far target was located 25° below the near target.
- (b) Far-up near-down (FUND): Subjects were asked to make self-paced shifts between the far and near targets, which were both continuously illuminated. The direction of the near target was at down 10° and the far target was located 25° above the near target.

3 Data analysis

In order to avoid aliasing, coil signals were passed through Krohn-Hite Butterworth filters (bandwidth, 0–150 Hz) before digitization at 500 Hz with 16-bit resolution. Conjugate eye position (version) was calculated from (right eye horizontal gaze + left eye horizontal gaze)/2. Vergence angle was calculated by subtracting right horizontal gaze from left horizontal gaze. Therefore, positive values indicate convergence and negative values indicate divergence. Eye position signals were differentiated (Ramat et al. 1999) to yield vergence velocity and vertical eye velocity signals, with noise typically less than $0.5^\circ/\text{s}$. Vergence (or saccadic) onset was defined as the time when vergence (or saccade) speed exceeded $10^\circ/\text{s}$, and the end as the time at which the speed dropped below $10^\circ/\text{s}$. Responses were analyzed interactively using programs written in MATLAB (The Mathworks Inc., Natick, MA, USA), to identify the time of start of the vergence movement, the time of start of the vertical saccade, the peak vergence velocity, the peak vertical saccade velocity, the times of peak vergence and vertical saccade velocities, the duration and size of the vergence movement and the duration and size of the vertical saccade. Transient, small divergence movements preceded most convergence responses (Maxwell and King 1992; Sylvestre et al. 2002) but, as shown in our prior study, did not impact on the responses that we measured. We defined skewness of the vergence velocity waveform as the ratio D_{acc}/D , where D_{acc} is the duration from onset of vergence movement to peak velocity, and D is the total duration of the vergence movement (van Opstal and van Gisbergen 1987).

4 Testing of models for saccade–vergence interactions

To test the model, we compared data from five subjects and modeled responses of only the convergence components, since these showed the largest differences in velocity waveform skewing for the two paradigms (Kumar et al. 2005). Five similar convergence responses for each subject were averaged for each of the two paradigms. Time arrays of 401 samples (representing a 0.8 s response time) of the convergence response were used as the data for the parameter estimation.

The SVBN model of Zee et al. (1992, see their Appendix) was coded in SIMULINK (The Mathworks Inc.). This model proposes that the vergence velocity command is generated by a pure vergence pathway summing with the SVBN pathway (activated by the omnipause neurons during combined saccade–vergence movements). The activity of convergence burst neurons of the SVBN pathway was modeled as an exponential; two parameters of this pathway, namely A , the asymptotic firing rate of the convergence velocity neurons and λ , the rate constant of firing, were estimated to find the most optimal fit to the data. Based on our present findings (see Sect. 5), we modified the SVBN model (Fig. 2b) such that a single pathway representing convergence velocity neurons generated the convergence velocity command. The shape of the nonlinearity representing activity of these neurons was assumed to be similar to that of the saccadic system (see Fig. 2b); four parameters of this nonlinearity were selected for optimization: A , the asymptotic firing rate of the convergence velocity neurons; λ , the rate constant of firing; int , the critical convergence motor error below which the firing pattern follows a linear rather than the exponential burst curve; and T_c , the time constant of the lag element that filters the output of the convergence velocity neurons.

Parameter estimation techniques provide a rigorous mathematical procedure to simultaneously estimate several parameters with precision. It has been previously applied to the study of eye movements (Huebner et al. 1990; Seidman et al. 1995; Das et al. 1998). Due to the complexity of the SVBN model, we did not attempt to write down the state equations describing the model; instead we took advantage of the seamless integration of SIMULINK with MATLAB (The Mathworks Inc.) to execute the model at each iterative step of the parameter estimation procedure. Parameter estimation was performed using the “lsqcurvefit” function of the MATLAB Optimization Toolbox (Coleman et al. 1999), which uses the method of conjugate gradients to minimize the objective function (Φ):

$$\Phi(B) = \sum [y_i - f_i(B)]^2 \quad (1)$$

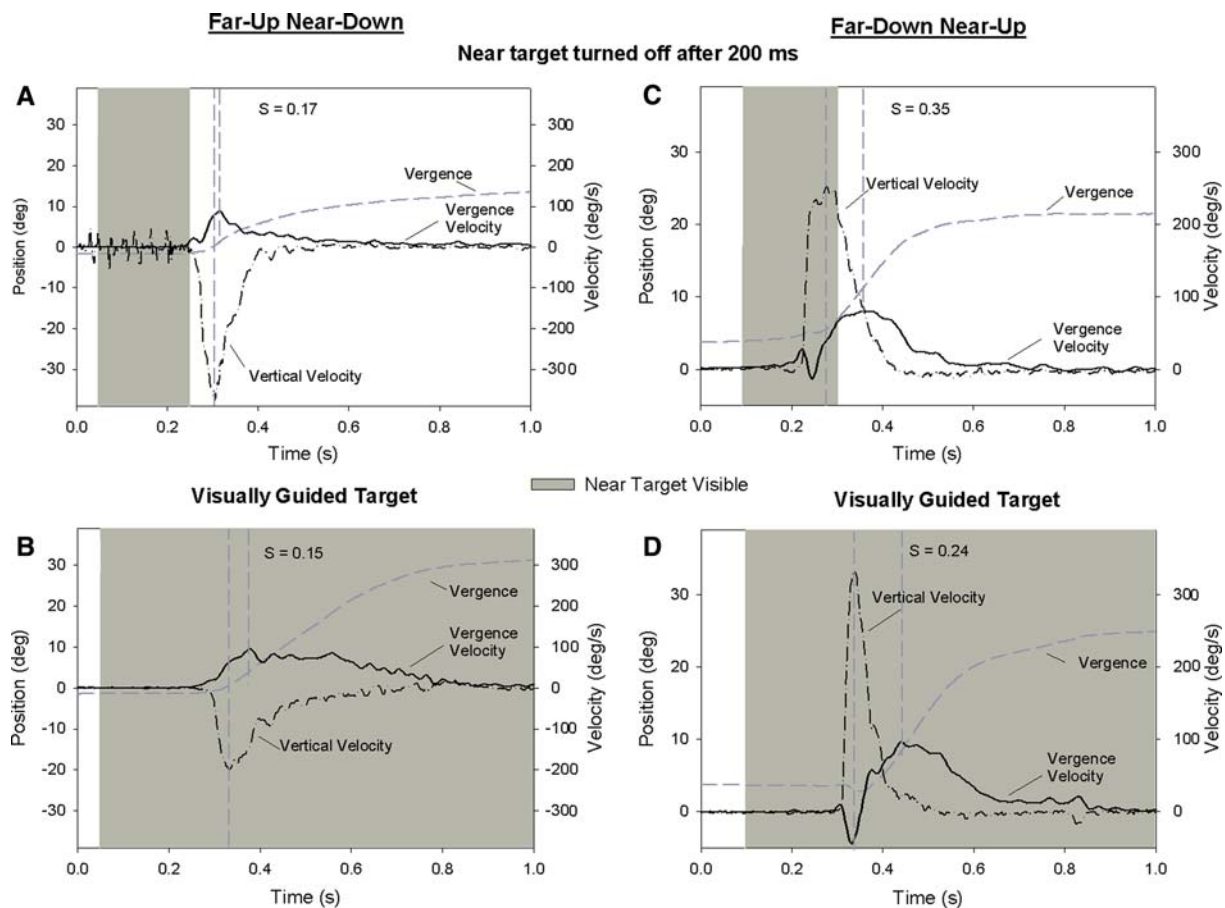


Fig. 3 Representative records from one subject of convergence movements made in concert with vertical saccades for the far-up near-down (FUND) and far-down near-up (FDNU) paradigms. **a** and **b** are convergence responses to the FUND paradigm, **c** and **d** are responses to the FDNU paradigm. The *top two panels*, **a** and **c**, show convergence responses when the near target was turned off after 200 ms and the subject was in total darkness so as to eliminate any possibility of visual feedback. The *bottom two*

panels, b and *d*, show visually-guided responses. Note how in both **a** and **b**, the responses remain highly skewed (skew ratio, $S < 0.17$), whereas in both **c** and **d**, the response has lesser skewing, indicating that skewing is not due to visual feedback. The velocity of the vertical saccadic component of the response is also provided and the *vertical dashed gray lines* indicate peak saccadic and vergence velocities, as in Fig. 1

where y_i are the measured data values, $f_i(B)$ are the calculated model output values, and B is the optimal parameter vector. The goal of the optimization algorithm is to minimize this objective function. The difference ($y_i - f_i$) is called the residual at time point t_i . For each estimate, different initial guesses were used to ensure the algorithm did not converge at local minima.

5 Results

5.1 Skewing of the convergence response

We first investigated whether the difference in skewing of the convergence velocity response during the two paradigms (FUND or FDNU) might be due to visual feedback. To supplement our prior study (Kumar et al. 2005), we compared both types of responses during

experiments when the visual targets were either continuously visible or the room was switched to darkness 200 ms after target presentation. For FUND responses, convergence waveforms remained more skewed than for FDNU responses, irrespective of whether the visual target was continuously visible or not (Fig. 3). Thus, differences in skewing could not be ascribed to visual feedback, and other factors must account for the difference of the two waveforms, which we investigated by testing whether the SVBN model by Zee et al. (1992) was able to accurately simulate these two types of responses.

5.2 The SVBN model

We averaged five similar representative saccade-convergence responses for each case (FDNU or FUND) for all five subjects; the convergence velocity components

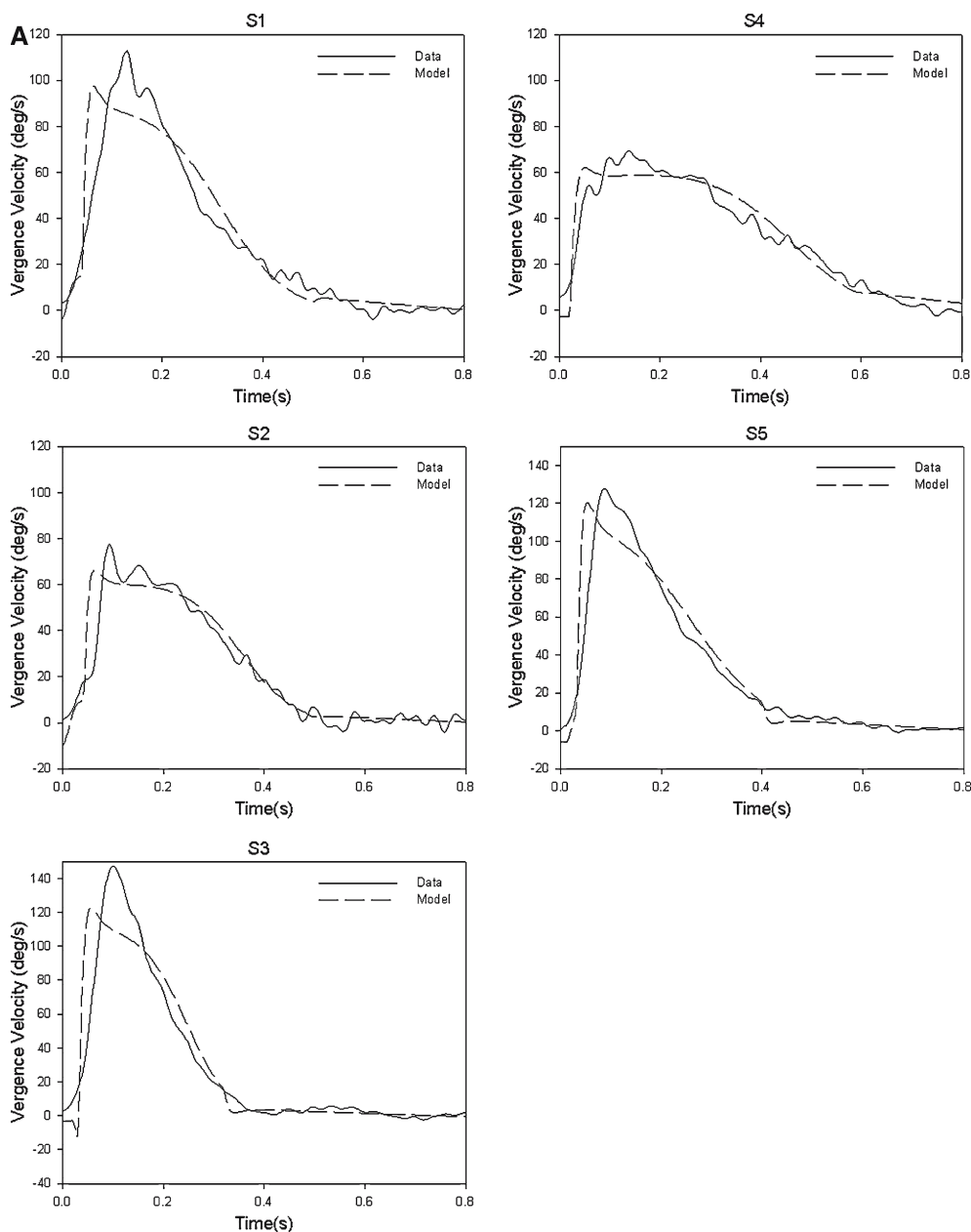


Fig. 4 Model simulations versus observed convergence responses for the SVBN model (Fig. 2a) during **a** FUNd and **b** FDNU paradigms for five subjects. Each data trace is an average of five similar responses aligned on the start of the convergence response.

are shown in Fig. 4 (solid lines). Figure 4 also shows the predicted output responses based on estimation of optimal parameters of the SVBN model (dashed lines). In the case of the FUNd responses (Fig. 4), the model accounted reasonably well for the observed response ($R^2 > 0.88$, sum of squared residuals $< 65\%$ – see Table 1). However, in the case of the FDNU responses (Fig. 4B), the model predictions were much less accurate ($R^2 < 0.91$, sum of squared residuals $> 100\%$, except in Subject 3, where the sum of squared residuals was 26.9%). The optimal parameter values and sum

of squared residuals are summarized in Table 1. Thus, although the SVBN model satisfactorily accounted for FUNd responses, it generally failed to do so for FDNU responses. Specifically, the model could not account for the decreased skewing that occurred with FDNU convergence responses.

of squared residuals are summarized in Table 1. Thus, although the SVBN model satisfactorily accounted for FUNd responses, it generally failed to do so for FDNU responses. Specifically, the model could not account for the decreased skewing that occurred with FDNU convergence responses.

5.3 Modification of the SVBN model

A major assumption of the SVBN model is that cessation of discharge of omnipause neurons is the mechanism by

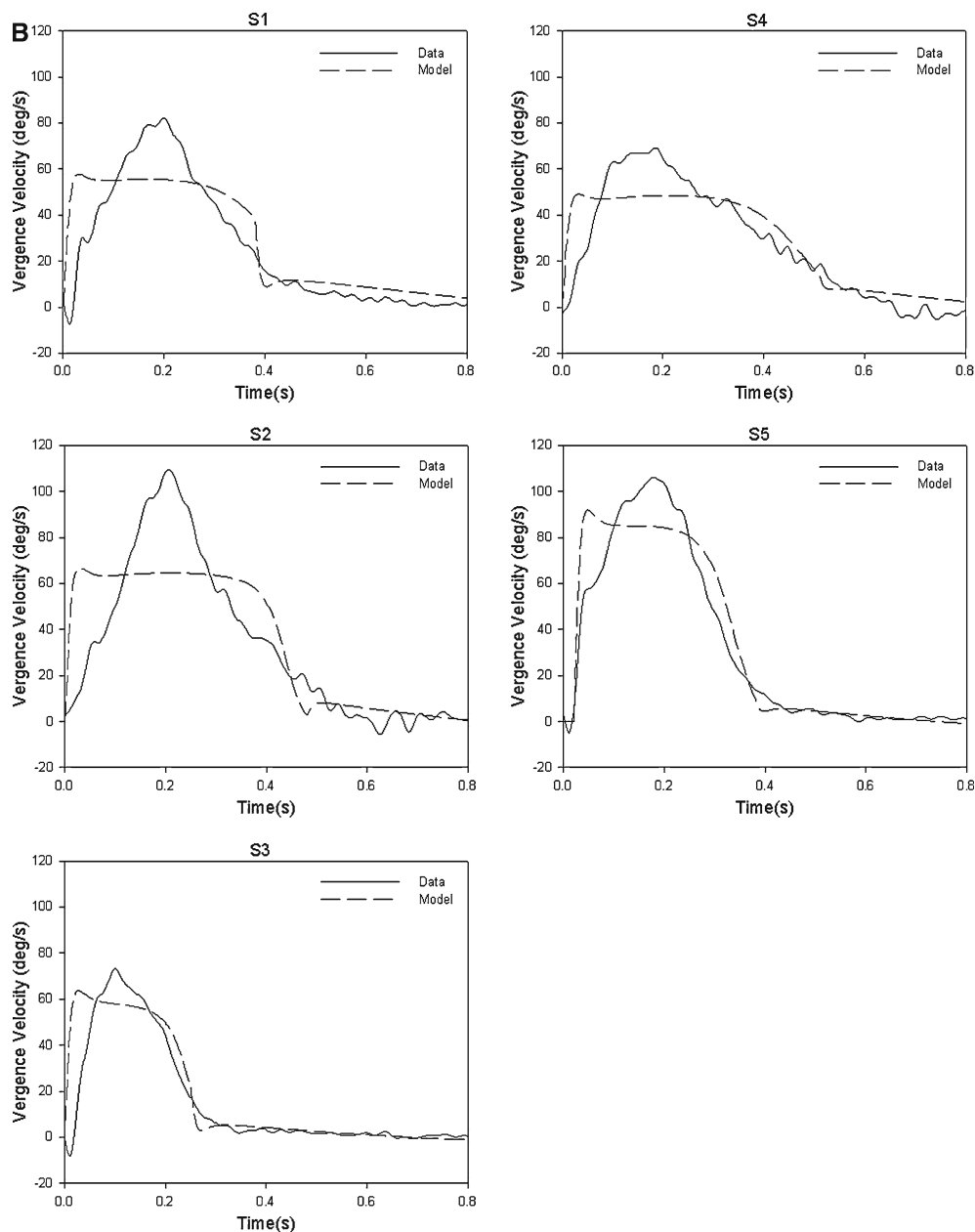


Fig. 4 (Contd.)

which vergence velocity is affected when accompanied by a saccade (Fig. 2). However, our present findings militate against this assumption. First, we found that convergence velocity showed a different velocity profile (less skewing) if convergence occurred after the saccadic component. Second, if low-amplitude, high-frequency conjugate oscillations are a marker that omnipause neurons are inhibited – a viewpoint supported by a number of studies (Ramat et al. 1999; Ramat et al. 2005; Zee et al. 1992) – then inhibition of omnipause neurons occurs during convergence responses to both the FDNU and FUND paradigms (Kumar et al. 2005). Thus, omnipause neurons appear to be inhibited irrespective

of the degree of skewing of the convergence velocity profile. Therefore, cessation of omnipause neuron discharge cannot solely account for the dynamic features of convergence that accompany saccades; the saccadic system must have another influence on the generation of the convergence motor command.

We propose that saccadic burst directly drives convergence burst neurons in a multiplicative manner (Fig. 2, asterisked arrow) – specifically, that the parameters of the convergence burst neurons are directly affected by the saccadic pulse. Thus, when convergence and saccadic components are synchronized, parameters describing discharge of convergence burst neurons

Table 1 Results of saccade-related vergence burst neuron (SVBN) model simulation

Parameter	Subject #1		Subject #2		Subject #3		Subject #4		Subject #5	
	FUND ($R^2 = 0.90$; RSS=64.3)	FUND ($R^2 = 0.75$; RSS=283)	FUND ($R^2 = 0.91$; RSS=23.4)	FUND ($R^2 = 0.67$; RSS=687)	FUND ($R^2 = 0.88$; RSS=62.7)	FUND ($R^2 = 0.79$; RSS=26.9)	FUND ($R^2 = 0.93$; RSS=40.1)	FUND ($R^2 = 0.79$; RSS=348)	FUND ($R^2 = 0.91$; RSS=49)	FUND ($R^2 = 0.91$; RSS=110)
Firing rate (A)	73.3	37.7	49.2	44.7	97.3	54.5	42.4	30.9	100.5	67.2
Rate constant (λ)	6.2	2.7	3.2	1.2	5.1	2.1	4.7	2.2	9.6	2.2

The optimal values for the parameters of the exponential nonlinearity of the SVBN model are shown for five subjects whose waveforms are plotted in Fig. 4, for both the far-up near-down (FUND) and the far-down near-up (FDNU) paradigms. Note that the fit is poor for the FDNU case in both subjects, as evidenced by the lower regression coefficient values (R^2) and the higher sum of squared residuals (RSS) between the velocity curves of the model output and the experimental data

will have a different set of values compared with when convergence follows the saccadic component. Like the SVBN model, our hypothesis incorporates a low-pass filter element. Simulations of this model are compared with observed responses and are summarized in Fig. 5. The new model generally made good predictions of both synchronized and dissociated convergence responses ($R^2 > 0.96$, sum of squared residuals $< 28\%$, except for the FDNU response of Subject 2 for which sum of squared residuals was 80.4%). Table 2 summarizes these results as well as optimal parameter values. Thus, this modified model could account for the range of skewing of convergence velocity waveforms encountered during both types of visual stimuli.

To gain an insight into the effect that each parameter exerted on the output of the model throughout the time course of the simulation, we plotted the sensitivity functions; Figure. 6a,c shows a plot of these functions for Subject 5. Due to the difference in scaling between the parameters, it appears that a unit change in T_c will influence the output of the model (Fig. 2) much more than, say, a unit change in λ . In order to better appreciate the relative contribution of each parameter toward the model output, we plotted the semi-relative sensitivity functions, obtained by scaling each sensitivity function by its corresponding optimal parameter value, (Fig. 6b,d). From these plots, we infer that the filter time constant T_c , has its effect mainly during the early part of the response, but plays a less significant role later in the response. This parameter also determines the rise time of the response. Overall, the parameters A , representing the asymptotic firing rate of the convergence velocity neurons, and λ , representing the rate constant of firing, contribute most strongly to the peak velocity of the response. The sensitivity function for the intercept (int) remains close to zero, indicating that the intercept does not play a major role in influencing

the convergence response for either paradigm. This also indicates that the model is quite insensitive to changes in the value of the intercept.

When the semi-relative sensitivity functions for each parameter are compared for FUND (more skewed) responses (Fig. 6b) versus FDNU (less skewed) responses (Fig. 6d), A , the asymptotic firing rate of the convergence burst neurons, and λ , the rate constant of the exponential curve that describes convergence burst neuron discharge show the greatest changes and could potentially contribute to the change in skewing of the convergence velocity waveforms. In comparison, T_c , the filter time constant, shows more modest changes.

To better understand this prediction of the model, we plotted the course of the convergence burst neuron nonlinearity with respect to the vergence motor error (VME in Fig. 2b), and compared it with the time course of the convergence velocity; an example is shown in Fig. 7. In the time plots, convergence velocity crosses the threshold ($10^\circ/\text{s}$) at points A and C, denoting the start and end of the convergence movement, respectively. Point B marks the occurrence of peak convergence velocity. These markers are also indicated on the nonlinearity profile curve. The arrows indicate the direction of change (increase or decrease) of the nonlinearity during the movement. The convergence burst neuron starts firing from near zero, and increases to a maximal value as the convergence motor error increases, corresponding to a step change in the required convergence angle. As the convergence movement starts, its velocity rises above the threshold (point A). The burst neuron firing then monotonically reduces as the convergence movement proceeds, as evidenced by the decrease in convergence motor error. Two differences are evident between the nonlinearity profiles for the two paradigms. First, for the FUND paradigm, the change in vergence motor error between A and B (corresponding to the

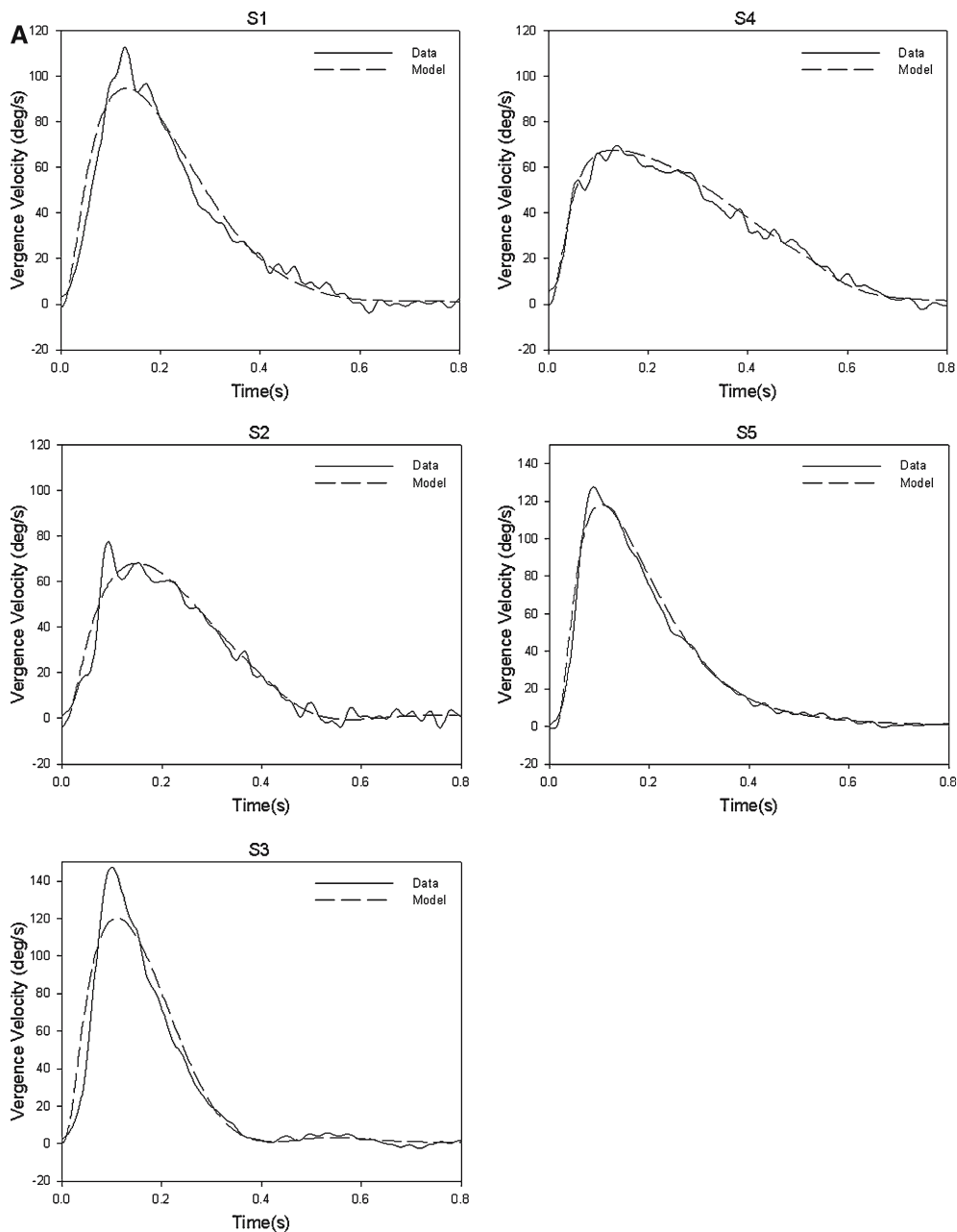


Fig. 5 Model simulations versus observed convergence responses for the modified SVBN model (Fig. 2) for **a** FUND and **b** FDNU paradigms for five subjects. Each data trace is an average of five similar responses aligned on the start of the convergence response.

Model simulations are with optimal parameters for the respective response. Note how the model and data traces overlap for responses to both **a** and **b**. See text for details

acceleration portion of the convergence response) is less than the change in convergence motor error between B and C (which corresponds to the deceleration portion of the convergence response). This implies that most of the convergence movement is accomplished in the deceleration portion of the response, leading to a skewed velocity profile. This differs from the FDNU case, where the change in convergence motor error

between A and B is more similar to the change in convergence motor error between B and C, resulting in a more symmetric velocity profile. Second, for the FUND paradigm, the burst neuron discharge reduces almost linearly between A and B, and between B and C. In contrast, for the FDNU paradigm, the discharge of the burst neuron changes very little between A and B, but drops sharply between B and C. Thus, the shape

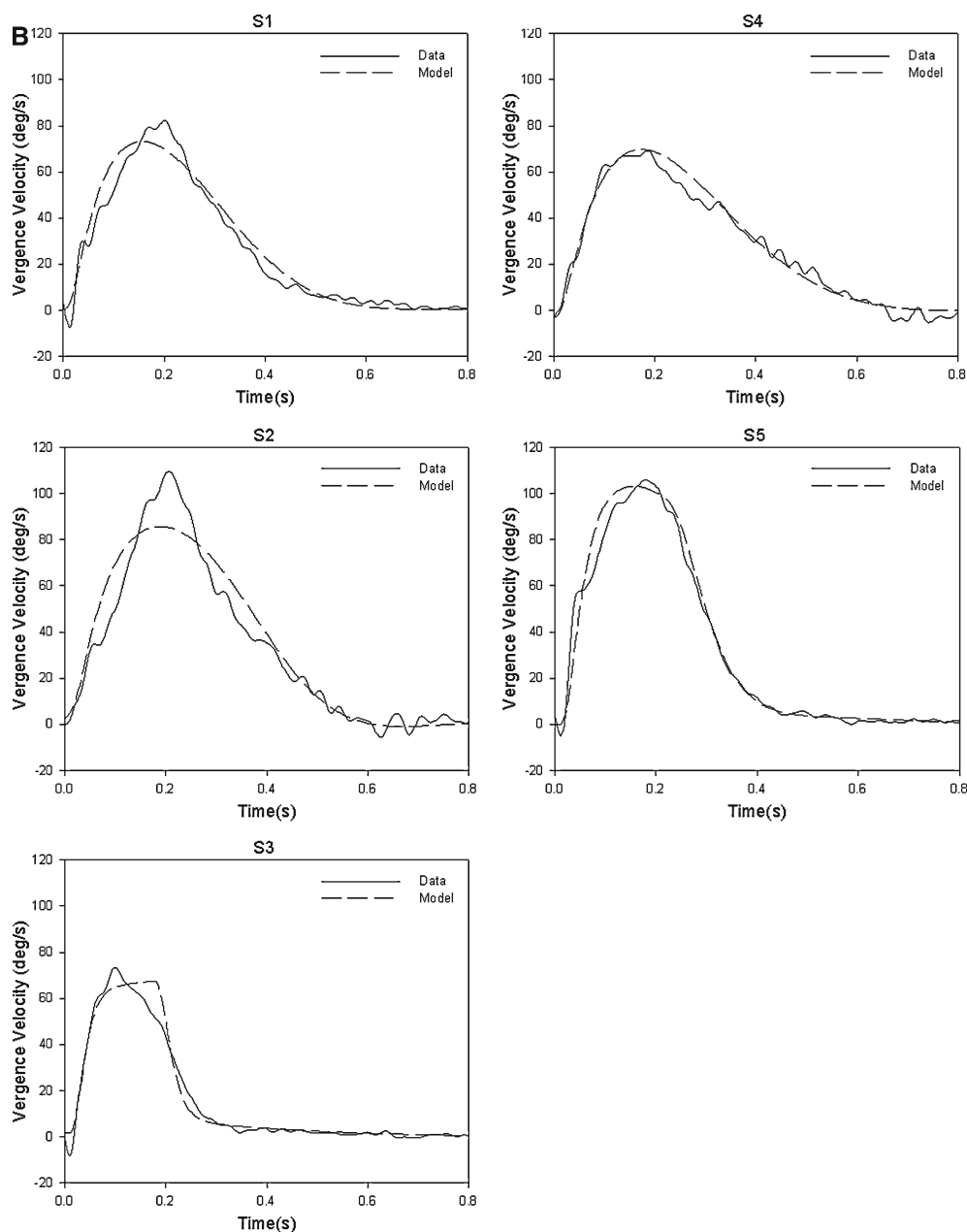


Fig. 5 (Contd.)

of the nonlinearity defining convergence neuron activity accounts for the different degrees of skewing of the velocity waveforms of these two responses. We postulate that the change in shape of the nonlinearity is caused by synchronous discharge of saccadic burst neurons, and develop this idea further in the following section.

6 Discussion

Using a novel finding from a prior study, we set out to test a model for saccade–vergence interaction. The behavior

used for testing this model was that, on the one hand, when a far stimulus lies above a near stimulus (FUND paradigm), convergence peak velocity follows vertical peak velocity by ~ 12 ms. On the other hand, when a far target lies below a near target (FDNU paradigm), convergence peak velocity follows the saccadic velocity peak by ~ 75 ms (Kumar et al. 2005). During the first, near-synchronous saccade–vergence response, the vergence velocity waveform was significantly more skewed than during dissociated responses. In our prior study, we systematically investigated the effects of vertical saccade size, horizontal vergence size, and orbital eye position

Table 2 Results of modified saccade-related vergence burst neuron (SVBN) model simulation

Parameter	Subject #1		Subject #2		Subject #3		Subject #4		Subject #5	
	FUND ($R^2 = 0.97$; RSS=21.7)	FUND ($R^2 = 0.96$; RSS=24.4)	FUND ($R^2 = 0.97$; RSS=2.92)	FUND ($R^2 = 0.93$; RSS=80.4)	FUND ($R^2 = 0.96$; RSS=27.7)	FUND ($R^2 = 0.97$; RSS=5.3)	FUND ($R^2=0.99$; RSS=13.1)	FUND ($R^2=0.98$; RSS=19.2)	FUND ($R^2=0.99$; RSS=4.3)	FUND ($R^2=0.98$; RSS=10.1)
Firing rate (A)	235.5	141.3	165.3	129	231.8	75.4	91.2	192.4	276.7	125.7
Rate constant (λ)	30	17.1	21.97	13.07	17.7	0.567	12.04	30	30	6.58
X-intercept (int)	0.098	0	0.669	0	0.075	2.65	1.16	0	0.12	0.04
Filter (T_c) time constant	0.046	0.055	0.056	0.062	0.036	0.013	0.025	0.07	0.025	0.027

The optimal values for the parameters of the modified SVBN model are shown for five subjects whose waveforms are plotted in Fig. 5, for both the FUND and the FDNU paradigms. Note that the fit is good for both paradigms in both subjects as evidenced by the high regression coefficient values (R^2) and the low RSS between the velocity curves of the model output and the experimental data

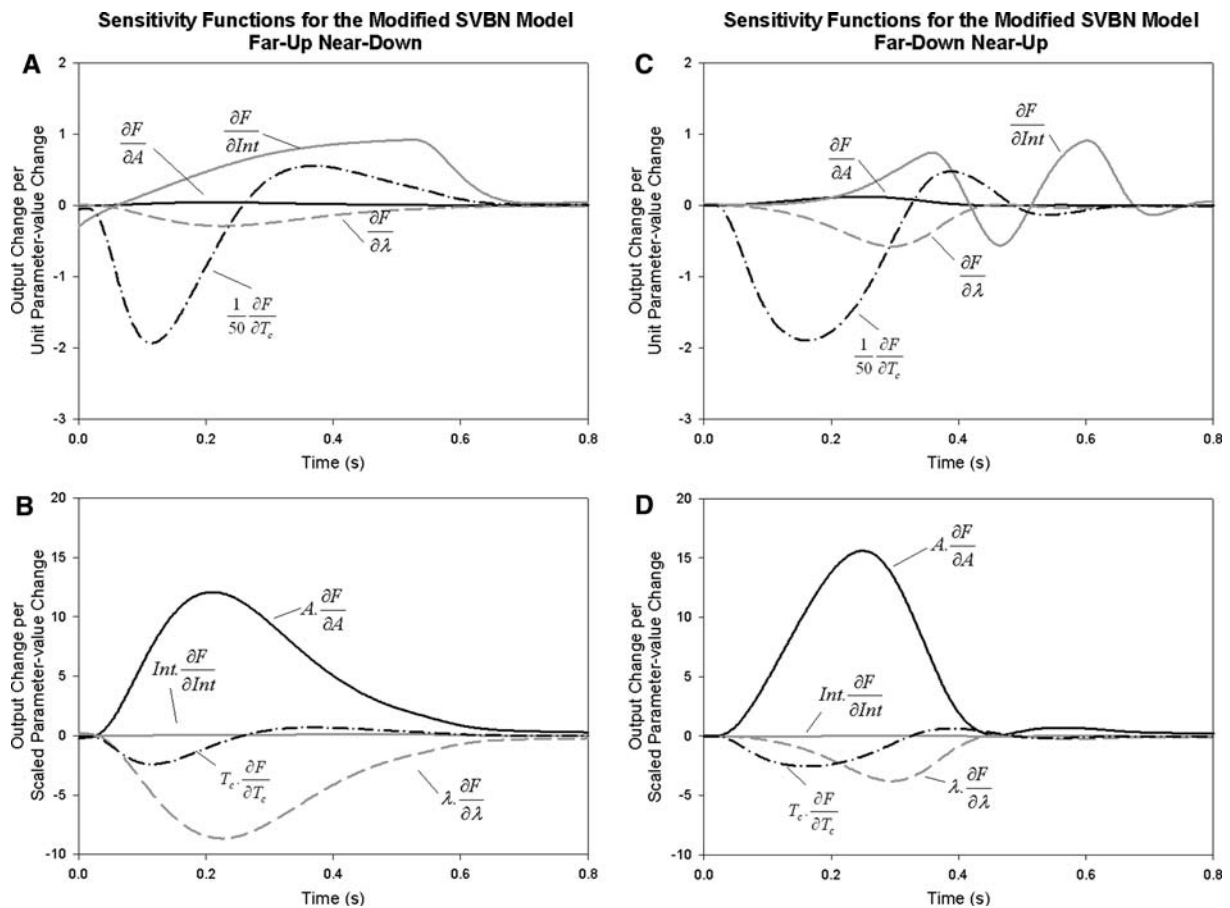


Fig. 6 Examples of parametric contributions to model simulation of responses from Subject 5. **a, c** Absolute sensitivity functions for the modified SVBN model, expressing change in output per unit-change in parameter value. **b, d** Semi-relative sensitivity functions expressing output change per scaled-unit-change in parameter value. *a* and *b* are for responses to the FUND paradigm, and *c* and *d* correspond to responses to the FDNU paradigm. F denotes the output of the model (convergence angle). $\partial F/\partial A$ rep-

resents the partial derivative of the model output with respect to the parameter A ; $\partial F/\partial \lambda$ represents the partial derivative of the model output with respect to the parameter λ ; $\partial F/\partial int$ represents the partial derivative of the model output with respect to the parameter int ; $\partial F/\partial T_c$ represents the partial derivative of the model output with respect to the parameter T_c . See text for details

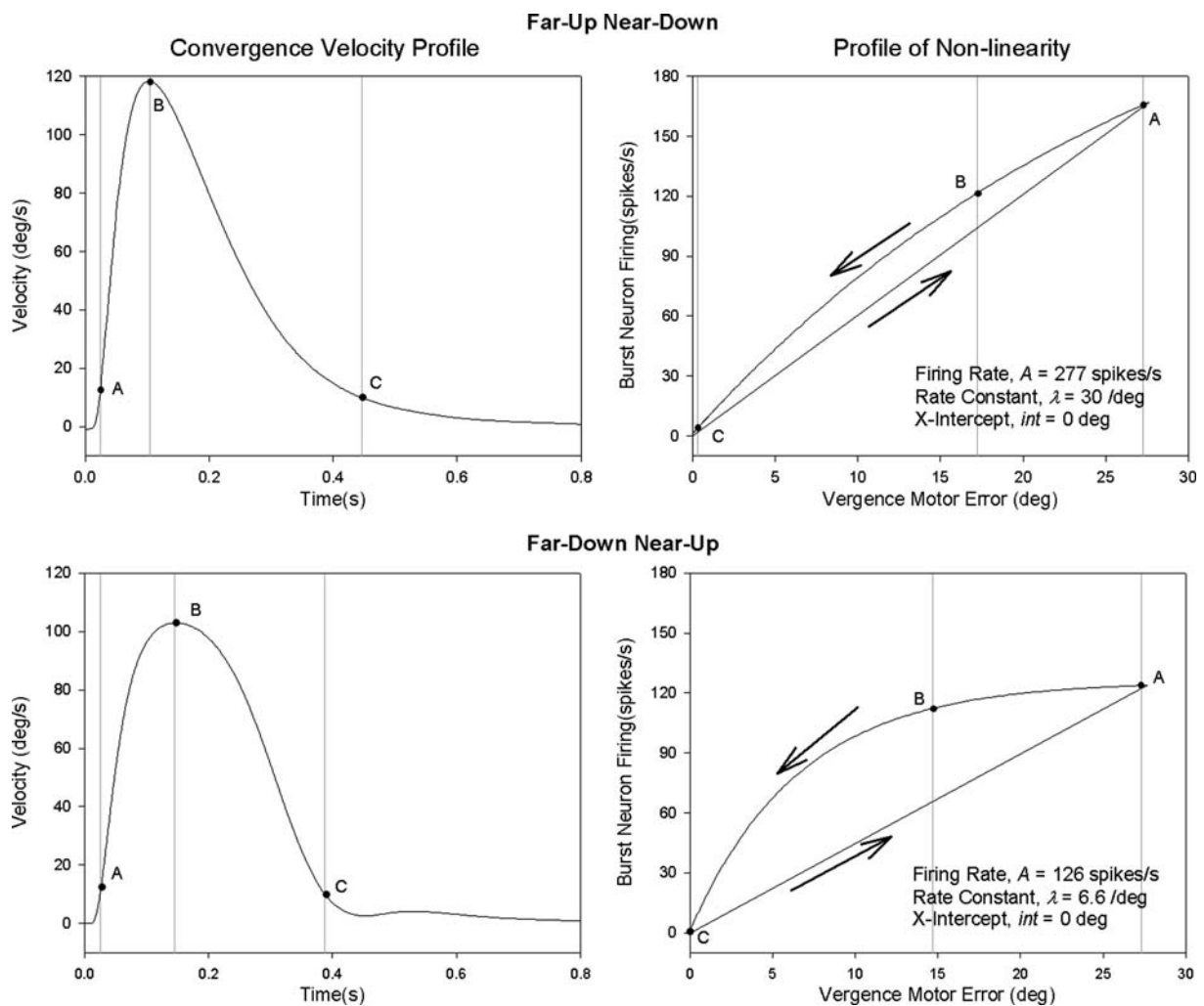


Fig. 7 Example comparing the time course of the convergence velocity profile and the course of the convergence burst neuron nonlinearity (data from Subject 5). The *panels on the left* show the convergence velocity profile. The convergence velocity starts (rises above the threshold of $10^\circ/s$) at point A, reaches a peak value at point B, and ends (falls below the threshold) at point C. The *panels on the right* plot the convergence burst neuron nonlinearity versus convergence motor error. The *arrows* indicate the temporal direction of change of the nonlinearity throughout the

vergence movement. The convergence burst neuron firing starts from near zero, and increases to the maximal (asymptotic) firing rate as the convergence motor error increases in response to a step change in the required convergence angle. The neuronal firing then decreases monotonically to zero as the convergence movement proceeds and convergence motor error reduces. *Points A–C* are markers that indicate events shown in the *left panels*. *Top panels* are for the FUND paradigm, and *bottom panels* are for the FDNU paradigm

at the end of the response, and concluded that the temporal dissociation of saccadic and vergence components was unlikely to be due to mechanical properties of the orbit. We also wondered if this skewing was due to visual feedback during the FUND paradigm. However, our control experiments indicated that the vergence system acted open-loop during both paradigms. Taking these findings together, we decided to investigate further central mechanisms that might govern the skewing of vergence components of combined saccade–vergence movements by testing current models for this behavior.

We found that the SVBN model described by Zee et al. (1992) could account for the vergence velocity waveform during the near-synchronized, but not the dissociated, responses. We were able to modify this model, so that vergence burst units changed their properties depending on whether a saccade occurred near-synchronously or not; this modified model accounted for both types of response. In discussing these findings, first, we consider possible mechanisms by which saccades may influence the dynamic properties of vergence movements, second, we address how the SVBN model might account for these mechanisms, and finally we suggest

general implications of the present study for development of alternative models for saccade–vergence interaction.

6.1 Possible mechanisms by which saccades may influence vergence

Assuming that there are separate saccadic and vergence systems, then the question arises: How do saccades affect vergence movements? (The converse question could also be asked, but it is not addressed in this paper). Our recent findings indicated that the dynamic properties of convergence and divergence are influenced by the direction and timing of the associated saccadic component. Saccades are known to speed up a range of other eye movements, including short-latency ocular following (Gellman et al. 1990), vergence (Busetini et al. 2001), and the onset of smooth pursuit (Lisberger 1998), although visual perturbations that simulate the effects of saccades have a similar effect. Other examples of “enhancement” of one type of eye movement by another include increased vestibulo-ocular reflex gain by a prior saccade (Das et al. 1999; Tabak et al. 1996). These effects might be due to a population of neurons that encodes both types of eye movements, such as the velocity-to-position neural integrator for eye movements (Cannon and Robinson 1985; Goldman et al. 2002). Interestingly, accommodation, like vergence, is also speeded up when it occurs in association with a saccade (Schor et al. 1999). Similar to this mechanism, the occurrence of a saccade might have a “multiplicative” effect on the output of the convergence-burst neurons without any intervention of the omnipause neurons (Busetini and Mays 2005). In our modeling efforts, we made a different suggestion: that the saccadic pulse transiently changed the values of parameters of the pool of convergence-generating neurons (Fig. 2, dashed arrow indicated by asterisk), when saccades and convergence movements were synchronized. In this way, discharge properties of vergence burst neurons would change to produce more or less velocity waveform skewing, depending on the timing and direction of an associated saccade. However, release of inhibition on convergence-burst neurons by omnipause neurons may still contribute to the effect of vergence enhancement.

6.2 Consideration of how the SVBN model might account for the present findings

An important difference between the SVBN model (Fig. a) and the model that we developed (Fig. b) is that, whereas the SVBN model has saccadic–vergence and smooth-vergence pathways, our model has only one

vergence pathway, the properties of which are influenced by a synchronous saccade. (Note, however, that a distributed, neural network model could incorporate neurons with a range of enhancements during saccades and this could be interpreted as being equivalent to two or more pathways.) While our model (Fig. b) simulates only combined saccadic–vergence movements, it seems possible that the convergence burst neurons may have different firing properties in the absence of a saccade, so that this model can be extended to simulate pure convergence responses. To describe the properties of the convergence pathway in our model, we chose a nonlinearity qualitatively similar to that postulated for saccades (van Gisbergen et al. 1981). However, this choice was arbitrary, and we found that the intercept of the exponential was not an important factor defining vergence behavior. Thus, other representations of the discharge of convergence neurons during saccades seem possible. Nonetheless, our model did provide an insight into the property of skewing of the convergence velocity waveform (Fig. 7). We found that the rate constant and asymptote governing the exponential curve largely determined the degree of skewing, with smaller rate constants and asymptote values (causing a longer plateau and steeper fall as the convergence motor error reduced) producing proportionally more skewing in four out of five subjects. It seems possible that similar factors contribute to the skewing that is observed for the velocity waveforms of larger saccades (van Opstal and van Gisbergen 1987). However, an alternative hypothesis is that a faster movement will reach its peak value earlier, allowing local feedback to guide the deceleration phase.

Currently, an anatomical substrate by which saccadic commands could influence vergence neuron activity is difficult to identify, although one possibility is neurons within the nucleus reticularis tegmenti pontis (NRTP). The NRTP contains vergence-related neurons and saccade-related neurons lying in close proximity (Gamlin 1995). It is also possible that vergence and saccadic commands might influence each within the superior colliculus (Chaturvedi and van Gisbergen 2000; Walton and Mays 2003), and the lateral intraparietal (LIP) area (Gnadt and Mays 1995). Through such connections, the high-frequency discharge of burst neurons in riMLF might influence horizontal convergence by changing the properties of midbrain vergence-generating neurons, when both systems are active at the same time (van Leeuwen et al. 1998). In our model, this would correspond to changes of parameter values, such as those shown in Fig. 6. Further studies are required to provide a firmer neurobiological substrate for the interaction between the saccadic and vergence systems.

6.3 Alternative models for saccade–vergence interactions

Our present study should be viewed in the overall context of current models for saccade-vergence interactions. Thus, both the SVBN model and the model that we propose are “Hering-type” models, which assume separate saccadic and vergence systems. A completely different view is embodied in “Helmholtz-type” models, in which saccadic burst neurons with monocular firing properties define disjunctive gaze shifts (King and Zhou 2002). This hypothesis proposes that monocular burst neurons could determine the dynamic properties of both conjugate components (similar discharge of bursters) and vergence components (difference in discharge between bursters). Electrophysiological evidence exists to support both Hering- and Helmholtz-type models, but interpretation of these data remains controversial (see, e.g., Mays et al. 1986; Zhou and King 1998; Mays 1998; Sylvestre and Cullen 2003). The novel visual stimulus that we applied in our human studies provides an opportunity to test these competing models, and preliminary results indicated that monkeys can be trained to carry out this task (K. E. Cullen, personal communication). Since the vergence and saccadic components are dissociated, electrophysiological studies may be able to determine whether the two components can be related either to separate vergence and saccadic burst generators, or rather to two temporally distinct bursts of activity by monocular saccadic burst neurons. Another issue concerns our using self-generated saccade–vergence responses to test the two models; although these were found to be dynamically similar to responses made to non-predictable jumps of a visual target (Kumar et al. 1995), different mechanisms are possible, even at a brainstem level. Finally, there is evidence that trochlear motoneurons decrease activity during convergence (Mays et al. 1991), and might, thereby contribute to the differences in vergence made with upward versus downward saccades. Testing this hypothesis requires further experiments that measure 3-D eye rotations.

Whatever model emerges from such studies, it must be able to account for the different dynamic properties of vergence during FUND and FDNU responses. If our hypothesis does turn out to be correct, it may be a specific example of a more general phenomenon. For example, neurologists often ask patients to carry out isometric contraction of upper limb muscles (“reinforcement” by the Jendrassik maneuver) in order to increase muscle tendon reflexes in the lower limbs. Similar strategies are evident in athletes as they strain to hone their performance. In this regard, the effects of vertical saccades

on the dynamic properties of horizontal convergence movements may provide an example of such reinforcement behavior that is accessible to electrophysiological investigation.

Acknowledgements This study is supported by NIH grant EY06717, NASA/NSBRI NA00208, the Office of Research and Development, Medical Research Service, Department of Veterans Affairs, and the Evenor Armington Fund (to Dr. Leigh). We are grateful to Drs. Kathleen Cullen, Jean Büttner-Ennever, Claudio Busettoni, Lance Optican, David Zee, John S. Stahl, and Dr. Gerald Saidel for helpful comments. The work reported in this paper constitutes research performed by Arun N. Kumar as part of the requirements for his Doctoral Dissertation.

References

- Busettoni, C, Mays LE (2003) Pontine omnipause activity during conjugate and disconjugate eye movements in macaques. *J Neurophysiol* 90:3838–3853
- Busettoni C, Mays LE (2005) Saccade-vergence interactions in macaque. II. Vergence enhancement as the product of a local feedback vergence motor error and a weighted saccadic burst. *J Neurophysiol* 94:2312–2330
- Busettoni C, FitzGibbon EJ, Miles FA (2001) Short-latency disparity vergence in humans. *J Neurophysiol* 85:1129–1152
- Cannon SC, Robinson DA (1985) An improved neural-network model for the neural integrator of the oculomotor system: more realistic neuron behavior. *Biol Cybern* 53(2):93–108
- Carpenter RHS (1991) The visual origins of ocular motility. In: Cronly-Dillon JR (ed) *Vision and visual function*, vol 8. Eye movements, MacMillan Press, London, pp 1–10
- Carpenter RHS (1988) *Movements of the eyes*. 2nd edn. Pion, London
- Chaturvedi V, van Gisbergen JAM (2000) Stimulation in the rostral pole of monkey superior colliculus: effects on vergence eye movements. *Exp Brain Res* 132:72–78
- Coleman T, Branch M, Grace A (1999) Optimization Toolbox for use with MATLAB, User's Guide. The Mathworks Inc., South Natick
- Collewijn H, Erkelens CJ, Steinman RM (1995) Voluntary binocular gaze-shifts in the plane of regard: dynamics of version and vergence. *Vision Res* 35:3335–3358
- Das VE, Dell'Osso LF, Leigh RJ (1999) Enhancement of the vestibulo-ocular reflex by prior eye movements. *J Neurophysiol* 81:2884–2892
- Das VE, DiScenna AO, Feltz A, Yaniglos S, Leigh RJ (1998) Tests of a linear model of visual-vestibular interaction using the technique of parameter estimation. *Biol Cybern* 78:183–195
- Enright JT (1984) Changes in vergence mediated by saccades. *J Physiol* 350:9–31
- Gamlin PDR, Clarke RJ (1995) Single-unit activity in the primate nucleus reticularis tegmenti pontis related to vergence and ocular accommodation. *J Neurophysiol* 73(5):2115–2119
- Gellman RS, Carl JR, Miles FA (1990) Short latency ocular following responses in man. *Visual Neurosci* 5:107–122
- Gnadt JW, Mays LE (1995) Neurons in monkey parietal area LIP are tuned for eye-movement parameters in three-dimensional space. *J Neurophysiol* 73(1):280–297
- Goldman MS, Kaneko CR, Major G, Aksay E, Tank DW, Seung HS (2002) Linear regression of eye velocity on eye position and head velocity suggests a common oculomotor neural integrator. *J Neurophysiol* 88:659–665

- Horn AKE, Büttner-Ennever JA, Suzuki Y, Henn V (1997) Histological identification of premotor neurons for horizontal saccades in monkey and man by parvalbumin immunostaining. *J Comp Neurol* 359:350–363
- Horn AKE, Büttner-Ennever JA (1998) Premotor neurons for vertical eye-movements in the rostral mesencephalon of monkey and man: the histological identification by parvalbumin immunostaining. *J Comp Neurol* 392:413–427
- Horn AKE, Büttner-Ennever JA, Wahle P, Reichenberger I (1994) Neurotransmitter profile of saccadic omnipause neurons in nucleus raphe interpositus. *J Neurosci* 14:2032–2046
- Huebner WP, Saidel GM, Leigh RJ (1990) Non-linear parameter estimation applied to a model of smooth pursuit eye movements. *Biol Cybern* 62:265–273
- King, WM, Zhou, W (2002) Neural basis of disjunctive eye movements. *Ann NY Acad Sci* 956:273–283
- Kumar AN, Han Y, Dell’Osso LF, Durand DM, Leigh RJ (2005) Directional asymmetry during combined saccade-vergence movements. *J Neurophysiol* 93: 2797–2808
- Leigh RJ, Zee DS (2006) *The neurology of eye movements*. 4th edn. Oxford University Press, New York
- Lisberger SG (1998) Postsaccadic enhancement of initiation of smooth pursuit eye movements in monkeys. *J Neurophysiol* 79(4):1918–1930
- Maxwell JS, King WM (1992) Dynamics and efficacy of saccade-facilitated vergence eye movements in monkeys. *J Neurophysiol* 68:1248–1260
- Mays LE (1984) Neural control of vergence eye movements: convergence and divergence neurons in the midbrain. *J Neurophysiol* 51:1091–1108
- Mays LE (1998) Has Hering been hooked? *Nat Med* 4:889–890
- Mays LE (2003) Neural control of vergence eye movements. In: Chalupa LM and Werner JS (eds) *The visual neurosciences vol 2*. MIT Press, Cambridge, pp 1415–1427
- Mays LE, Gamlin PDR (1995) A neural mechanism subserving saccade-vergence interactions. In: Findlay JM, Walker R, Kentridge RW (eds) *Eye movement research: mechanisms, processes and applications*, Elsevier, Amsterdam, pp 215–223
- Mays LE, Porter JD, Gamlin PDR, Tello C (1986) Neural control of vergence eye movements: neurons encoding vergence velocity. *J Neurophysiol* 56:1007–1021
- Mays LE, Zhang Y, Thorstad MH, Gamlin PD (1991) Trochlear unit activity during ocular convergence. *J Neurophysiol* 65:1481–1491
- Ramat S, Leigh RJ, Zee DS, Optican LM (2005) Ocular oscillations generated by coupling of brainstem excitatory and inhibitory saccadic burst neurons. *Exp Brain Res* 160:89–106
- Ramat S, Somers JT, Das VE, Leigh RJ (1999) Conjugate ocular oscillations during shifts of the direction and depth of visual fixation. *Invest Ophthalmol Vis Sci* 40:1681–1686
- Schor CM, Lott LA, Pope D, Graham AD (1999) Saccades reduce latency and increase velocity of ocular accommodation. *Vision Res* 39:3769–3795
- Seidman SH, Leigh RJ, Tomsak RL, Grant MP, Dell’Osso LF (1995) Dynamic properties of the human vestibulo-ocular reflex during head rotations in roll. *Vision Res* 35:679–689
- Sparks DL (2002) The brainstem control of saccadic eye movements. *Nat Rev Neurosci* 3: 952–964
- Sylvestre PA, Galiana HL, Cullen KE (2002) Conjugate and vergence oscillations during saccades and gaze-shifts: Implications for integrated control of binocular movement. *J Neurophysiol* 87:257–272
- Sylvestre PA, Cullen KE (2003) Dynamics of abducens nucleus neuron discharges during disjunctive saccades. *J Neurophysiol* 88:3452–3468
- Tabak S, Smeets JB, Collewyn H (1996) Modulation of the human vestibuloocular reflex during saccades: probing by high-frequency oscillation and torque pulses of the head. *J Neurophysiol* 76:3249–3263
- van Gisbergen JAM, Robinson DA, Gielen S (1981) A quantitative analysis of the generation of saccadic eye movements by burst neurons. *J Neurophysiol* 45:417–442
- van Leeuwen AF, Collewyn H, Erkelens, CJ (1998) Dynamics of horizontal vergence movements: interaction with horizontal and vertical saccades and relation with monocular preferences. *Vision Res* 38:3943–3954
- van Opstal AJ, van Gisbergen JAM (1987) Skewness of saccadic velocity profiles: a unifying parameter for normal and slow saccades. *Vision Res* 27:731–745
- Walton MMG, Mays LE (2003) Discharge of saccade-related superior colliculus neurons during saccades accompanied by vergence. *J Neurophysiol* 90:1124–1139
- Yoshida K, Iwamoto Y, Chimoto S, Shimazu H (1999) Saccade-related inhibitory input to pontine omnipause neurons: an intracellular study in alert cats. *J Neurophysiol* 82:1198–1208
- Zee DS, FitzGibbon EJ, Optican LM (1992) Saccade-vergence interactions in humans. *J Neurophysiol* 68:1624–1641
- Zhou W, King WM (1998) Premotor commands encode monocular eye movements. *Nature* 393:692–695